Activity for Diesel Particulate Matter Oxidation of Silver Supported on Al_2O_3, TiO_2, ZnO, and CeO_2: The Effect of Oxygen Concentration

Punya Promhuad[1], *Boonlue* Sawatmongkhon[1,2,*], *Nuwong* Chollacoop[3], *Kampanart* Theinnoi[1,2], *Thawatchai* Wongchang[2,4] and *Ekachai* Juntasaro[5]

[1] College of Industrial Technology, King Mongkut's University of Technology North Bangkok, 1518 Pracharat 1 Road, Wongsawang, Bangsue, Bangkok 10800, Thailand.
[2] Research Centre for Combustion Technology and Alternative Energy (CTAE), Science and Technology Research Institute, King Mongkut's University of Technology North Bangkok, Bangkok 10800, Thailand.
[3] Renewable Energy and Energy Efficiency Research Team, National Energy Technology Center (ENTEC), 114 Thailand Science Park, Klong Luang, Pathumthani 12120, Thailand.
[4] Department of Mechanical and Automotive Engineering Technology, Faculty of Engineering and Technology, King Mongkut's University of Technology North Bangkok (Rayong Campus), Rayong 21120, Thailand.
[5] The Sirindhorn International Thai-German Graduate School of Engineering (TGGS), King Mongkut's University of Technology North Bangkok, 1518 Pracharat 1 Road, Wongsawang, Bangsue, Bangkok 10800, Thailand.

Abstract. Particulate matter (PM) is a problem for human health the major producer of PM are diesel engines. The diesel particulate filters (DPFs) are used for the limitation of the PM. The DPF operation consists of two sequential functions: PM filtering and regeneration. One of the main contributing factors affecting the regeneration of DPF is the oxygen concentration in the exhaust gas. This study investigates the impact of different oxygen concentrations (99.99%, 10%, and 5%) on (PM) oxidation when using silver catalysts supported on CeO_2, ZnO, TiO_2, and Al_2O_3. The synthesized catalysts were characterized using XRD, SEM, SEMEDX, and H_2-TPR techniques, and the PM oxidation activity was evaluated using TGA. The results demonstrated that different oxygen concentrations had little effect on light VOCs oxidation compared to no catalyst or the same catalyst. However, heavy VOCs and soot combustion, which require a higher oxygen concentration, significantly reduce combustion performance when the oxygen concentration decreases.

Keyword. Al_2O_3, CeO_2, Oxygen concertation, PM oxidation, Silver catalyst, TiO_2, ZnO

1 Introduction

Air pollution is a significant environmental issue that adversely impacts human health [1], especially, the respiratory system, which could be damaged by the smaller size of particulate matter like inhalable PM_{10} (particulate matter with an aerodynamic diameter ≤ 10 μm,) and fine $PM_{2.5}$ [2]. Internal combustion engines, particularly diesel engines, are today a major producer of PM [3]. To mitigate this issue, the use of diesel particulate filters (DPFs) has emerged as a viable solution. The function of DPF comprises two main stages: filtration and regeneration [4]. During the filtration phase, particulate matter (PM) particles are trapped by the permeable structure of the diesel particulate filter (DPF), after which the accumulated PM is subjected to oxidation by oxygen at elevated temperatures, typically exceeding 600 ºC, during the regeneration phase [5-7]. However, the temperature of exhaust gas produced by a diesel engine is normally less than 600 ºC [8,9], so the exhaust gas cannot successfully be oxidized.

The application of catalyzed diesel particulate filter (cDPF) technology has been shown to reduce the temperature of regeneration [10]. Oxidation catalysts, typically composed of noble metals such as platinum (Pt), palladium (Pd), and silver (Ag), supported on metal oxide materials including ceria (CeO_2), alumina (Al_2O_3), and silica (SiO_2) [11-13]. Incorporating an oxidation catalyst can significantly lower the activation energy required for PM oxidation, thereby enabling combustion to occur at lower temperatures. Ag is well-known as a potential oxidation catalyst among the various noble metals [5]. Zhang and Jiang [5] studies revealed that Ag catalysts facilitate the synthesis of adsorbed active oxygen species such as peroxide (O_2^{-2}) and superoxide (O_2^-), also exhibit oxidative stability, which is crucial for Ag efficacy in promoting PM oxidation [11]. Moreover, Ag is a more affordable and cost-effective alternative for oxidation catalyst use than other noble metals [14].

* Corresponding author: boonlue.s@cit.kmutnb.ac.th

The support material has an important role in promoting PM combustion. Using alumina as a support material for oxidation catalysts, for example, Pt [15] and Ag [16], has been a good promoter for soot oxidation. Aneggi *et. al*., [17] described the behavior of silver deposited on ceria in the oxidation of carbon soot particulate. The research was further expanded to include additional supports such as alumina and zirconia, which have been shown to be effective in numerous Ag oxidation processes. The addition of Ag to ZrO_2 or Al_2O_3 resulted in strong soot oxidation activity in both fresh and aged conditions. TiO_2 emerged as an additional oxide support material that demonstrated effectiveness in promoting particulate matter (PM) oxidation. This efficacy can be attributed to its notable surface area, optimal dispersion of the metal catalyst, and robust metal-support interaction (SMSI), thereby augmenting the catalytic activity. [18]. Ceria is one of the silver catalysts' most commonly used support materials due to its redox properties and oxygen storage capacity (OSC) [13]. The redox properties (the switching of Ce^{3+} to Ce^{4+}) promote high OSC performance [13], resulting in an increase in soot oxidation performance. The increase in oxygen vacancy due to a decrease in lattice oxygen also contributes to the soot oxidation activity [19]. The mechanisms of soot oxidation using CeO_2-based catalysts involve two consecutive steps [20,21]. First, the soot is combusted by lattice oxygen (OL), which affects the formation of oxygen vacancy (Ov) and reduces CeO_2 (Ce^{4+}) to CeO (Ce^{3+}). Then, the gas-phase oxygen adsorbs on the surface of CeO_2 and transforms into active oxygen [22].

The performance of PM oxidation was promoted by noble metals and supporters. Additionally, the oxygen concentration is the primary influence on effect the of PM oxidation performance. Zhao *et. al*., [23] examined the combustion characteristics of soot and the impact of oxygen concentration and regeneration temperature on the continuous pulsation regeneration of a DPF. The study found that oxygen concentration is a highly effective indicator of regeneration efficiency, and that oxygen is the primary reactant in the soot regeneration reaction. In other words, the level of oxygen in the DPF directly affects the conditions necessary for successful soot combustion. The above research shows that oxygen concentration affects PM combustion when using Ag on different oxide supporters. It may be showing different promotions of PM combustion and its effect on PM oxidation performance. This paper aims to study the oxygen concentrations that impact PM oxidation performance when using silver catalysts on different oxide support (eg. CeO_2, ZnO, TiO_2, and Al_2O_3).

2 Experimental

2.1 Catalyst and Particulate matter preparation

This study's incipient wetness impregnation method employed the silver medal as a catalyst on four distinct supports. The synthesis process was initiated by dissolving silver nitrate (sourced from Thomas Baker Chemicals, India) in an appropriate quantity of distilled water, aiming to attain a silver loading of 16 wt% on the respective support materials. This study used 16wt% of Ag because of previous research conducted by our research group, which indicated that a 16 wt% Ag concentration on Al_2O_3 exhibited the best at promoting PM combustion [11]. The support materials employed in this study encompassed γ-alumina (sourced from Ajax Finechem, Australia) with a BET surface area measuring 142 m^2/g, titanium oxide (obtained from KEMAUS, Australia), and zinc oxide (procured from Quality Reagent Chemical, New Zealand). For ceria, a silver concentration of 5 wt% of the weight of CeO_2 was employed, as this concentration was determined to be conducive to promoting effective calcination. This study used 5wt% of Ag with CeO_2 as it is the best to promotes soot oxidation [13]. In this research, oxide supports were selected as representatives of different support material groups. For instance, Al_2O_3 was chosen as a representative of acidic support materials. TiO_2 (anatase structure) was selected as a representative of support materials classified as oxide semiconductors. ZnO was chosen as a representative of group II-VI semiconductor support materials. Lastly, CeO_2 was selected as a representative of reducible support materials. Subsequently, the precursor-laden supports were dried in an oven at 110 ºC overnight and then calcined in static air at 600 ºC for 2 h to obtain the final calcined samples.

The gaseous emissions generated by a diesel engine were employed as a direct reservoir for the retention of PM. The engine was operated under controlled conditions with varying speeds ranging from 1000 to 2000 rpm and loads ranging from 25% to 75% of the maximum load. To facilitate the experimental setup, a stainless-steel mesh with a mesh count of 500 per square inch was strategically placed inside the exhaust pipe, which possessed an inner diameter of 50 mm. The mesh was carefully rolled in a unidirectional manner for optimal positioning and effectiveness. The PM particles were trapped on the mesh and subsequently collected. The collected PM was then dried in a furnace at 110 ºC for 8 h. For future studies, the dried PM was stored in an airtight container.

2.2 Material characterisation

The X-Ray Diffraction (XRD) patterns of the synthesized catalysts were examined using a Rigaku Miniflex 600 diffractometer (manufactured by Rigaku, Japan), with Cu-Kα radiation (λ = 1.5418 Å) employed as the X-ray source. The diffractograms were recorded within the angular range of 10º to 80º at a scanning rate of 2º/min. The average sizes of the crystallites were determined using Scherrer's equation. The catalysts underwent examination and characterization utilizing a ZEISS AURIGA field emission scanning electron microscope (FE-SEM) equipped with an Oxford Instruments energy-dispersive X-ray (EDX)

spectrometer. This analytical setup allowed for the acquisition of microscopic images and the analysis of elemental compositions. The reducibility of the catalysts was investigated using H_2 temperature-programmed reduction (H_2-TPR) analysis. The measurements were performed using a ChemiSorb 2750 instrument (Micromeritics, United States) equipped with a thermal conductivity detector (TCD). Approximately 60 mg of the catalyst sample was loaded into a quartz reactor and subjected to a controlled temperature ramp. A gas mixture of 10 vol.% H_2 in He, flowing at a rate of 30 ml/min, was passed over the sample. The temperature was gradually increased from room temperature to 800 °C at a heating rate of 10 °C/min. The data were collected during the temperature ramp ranging from 80 °C to 700 °C.

2.3 Catalytic activity tests

The catalytic oxidation activity of PM was assessed using thermogravimetric analysis (TGA) with a PerkinElmer® Pyris 1 instrument. Prior to analysis, the PM samples were mixed with the catalyst at a predetermined weight ratio of 1/5. To ensure proper blending and close contact between the PM and catalyst, a stainless-steel mortar was employed for a 5-min duration. Next, an aliquot of approximately 10 mg from the prepared mixture was carefully transferred into a ceramic crucible. The temperature of the crucible was gradually raised from ambient temperature to 110 °C at a controlled heating rate of 10 °C/min, while maintaining a continuous flow of nitrogen gas. Subsequently, the purge gas was switched to oxygen (O_2) to facilitate the oxidation process, and the temperature was further increased to 700 °C, following the same heating rate of 5 °C/min. The purity of the oxygen was 99.99%, with concentrations of 10 vol.% O_2 in N_2 and 5 vol.% O_2 in N_2, flowing at a constant rate of 50 cm^3/min. The selection of oxygen concentration is necessary to align with the oxygen concentration within the exhaust gas of a diesel engine, which typically ranges from 5-17 vol% depending on the engine load [24,25]. However, in the exhaust gas of a diesel engine using biodiesel as fuel, the oxygen concentration is typically around 10 vol.% [26,27]. Based on these reasons, a concentration of 10 vol.% was chosen as the representative oxygen concentration derived from actual combustion in the engine. Additionally, a concentration of 5 vol% was selected as it represents the minimum concentration observed from combustion in a diesel engine, aiming to investigate the worst-case scenario of combustion. Lastly, the selection of a 99.99 vol.% concentration was made to examine the best performance of PM combustion. Continuous recording of sample weight was performed during the temperature ramp to monitor changes. PM oxidation activity was assessed based on several parameters. T_{20} corresponds to the temperature at which complete combustion of light volatile organic compounds (VOCs) occurs, defined as a 20% weight loss from the initial mass. T_{55} represents the temperature at which a 55% weight loss occurs from the initial mass, indicating the complete combustion of the heavy VOCs contained in the PM [11]. Finally, T_{90} is the temperature at which a 90% weight loss is observed and is used as an indicator of the performance of soot.

3 Result and discussion

A section of the results and discussion will show the result of the materials characterization, the PM oxidation activity and PM oxidation performance. The materials characterization shows the XRD result, SEM EDX image, and reducibility (H_2 -TPR). The TGA analyzer was used to define the PM oxidation activity and PM oxidation performance. The result and discussion of the PM oxidation activity show the activity when using different supporters and concentrations of oxygen. The silver used the different oxide supporters as follows: Al_2O_3, TiO_2, ZnO and CeO_2. The concentration of oxygen used was 99.99 %, 10 and 5 %vol of N_2.

3.1 The materials characterization

3.1.1 XRD

Figure 1 shows the XRD profiles of Ag on four supporters in this work. The 2Θ of metallic silver (JCPDS 04-0783) shows at 38.2°, 44.4°, 64.5°, 77.3°, and 81.4° indicate the (1 1 1), (2 0 0), (2 2 0), (3 1 1), and (2 2 2) [28,29]. The result in this work shows the same angle diffraction of Ag on all the oxide supporters except the case of Ag/CeO_2. As the Ag on the Ag/CeO_2 is 5 % by weight, it makes the small peak of silver for diffraction.

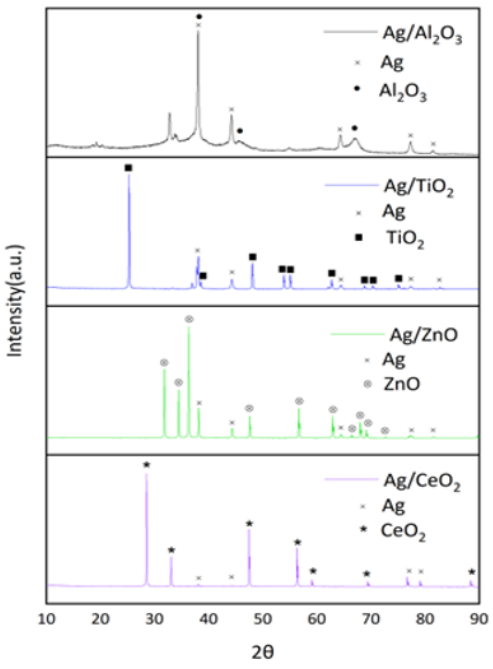

Fig. 1. The XRD profiles for Ag/Al_2O_3, Ag /TiO_2, Ag/ZnO and Ag/CeO_2.

The diffraction peak of Al_2O_3 (γ-Al_2O_3) was shown in the case of Ag/Al_2O_3, which is around 39.5°, 45.8°, and 67° [18]. Ag/TiO_2 shows the diffraction peaks of titanium the type anatase, which were angles at 25.64°, 38.26°, 48.40°, 63.00°, 69.26°, and 75.16° [26,27]. Corro *et. al*., [30] used the XRD technique to identify the peaks of ZnO. The authors presented peaks at 32°, 34°, 36°, 47°, 56°, 63°, 66°, 68°, and 69o, which provided insights into the structural characteristics of ZnO as same in the case of Ag/ZnO of this work. Ag/CeO_2 showed the peaks of Ceria at 28.5° (1 1 1), 33.1° (2 0 0), 47.5° (2 2 0), 56.3° (3 1 1), 59.1° (2 2 2), 69.3° (4 0 0), 76.6° (3 3 1), 79.1 (4 2 0), and 88.5 (4 2 2). The mean Ag^0 crystallite size across each catalyst demonstrates that diverse supports have distinct impacts on the dispersion of the active metal and its interaction with the support material. The ascending sequence of average crystallite sizes of Ag^0 on different supports is as follows: Ag/Al_2O_3 (11 nm), Ag/TiO_2 (13 nm), Ag/ZnO (15 nm), and Ag/CeO_2 (41 nm).

3.1.2 SEM and SEM EDX

Figure 2 shows SEM and SEM EDX which present the element of catalyst and supporter. In the first group (i), the catalytic and supporter morphology is demonstrated with the following images: Ag/Al_2O_3 (a,i), Ag/TiO_2 (b,i), Ag/ZnO(c,i), and Ag/CeO_2 (d,i). The second group (ii) shows the composition of the support, which includes Al(a,ii), Ti (b.ii), Z(c,ii), and Ce(d,ii). Oxygen elements in all support materials are shown in group (iii) images. Finally, in group (iv) images, the dispersion of Ag on each support material is demonstrated, as follows: Ag/Al_2O_3 (a,iv), Ag/TiO_2 (b,iv), AgZnO (c,iv), and Ag/CeO_2 (d,iv). The SEM EDX images clearly show different Ag dispersions on different support materials. Moreover, it is evident that the Ag particles exhibit a greater size and increased agglomeration in the scenarios involving Ag/TiO_2 and Ag/ZnO catalysts, in comparison to the Ag/Al_2O_3 catalyst. The size of the catalyst particles may also influence the circumstances of interaction between the catalyst and the soot [31]. The small-sized catalyst particles have a large surface area, resulting in close or excellent contact conditions [11,35]. In the case of Ag/CeO_2 shows a low density of silver, which compare with another case because the perpetration of Ag is 5 wt% that it is lower than another support. The findings of the SEM EDX investigations agreed well with the XRD results.

3.1.3 H_2-TPR

Figure 3 shows the H_2 profile of Ag on several oxide supporters in each temperature range. The oxidation activity was promoted by active oxygen species from both the surface and lattice oxygen. The active oxygen species could respond with H_2. For example, the surface oxygen on Ag_2O responds with H_2 as follows: $Ag_2O+H_2 \rightarrow 2Ag^0+H_2O$ [3]. The consumption of H_2 was shown by a peak of the TCD signal in H_2-TPR. It is well known that the temperature was higher than 300 °C, Ag_2O completely changed to Ag^0 [33].

The TCD signal for Ag/CeO_2 exhibited two distinct peaks. The first peak, observed at 190 °C, indicated the consumption of H_2 by the surface oxygen of the material. The presence of Ag_2O was found to facilitate the reaction with H_2. Additionally, a surface reaction between H_2 and CeO_2 was observed, resulting in the formation of oxygen vacancies on the ceria surface. The second peak in the TCD signal is detected at a temperature of 700 °C, which exceeded the combustion range of particulate matter.

Ag/ZnO shows two distinct peaks in the TCD signal at temperatures of 212 °C and 600 °C, respectively. These peaks indicated the consumption of H_2 through active oxygen species from both surface and lattice oxygen. The surface oxygen was replenished by Ag_2O when the temperature was below 300 °C, while the lattice oxygen was released from ZnO. The reaction involved the reduction of Zn^0 to Zn^+, as expressed by the equation: $ZnO + H_2 \rightarrow Zn^0+H_2O$, which was catalyzed by metallic copper (Cu) [34]. The results obtained for Ag/ZnO are consistent with those reported by Zhao et al. [35], who observed only a single peak in the TCD signal at 600 °C.

Ag/TiO_2 shows the single peak in the TCD signal at a temperature of 176 °C, indicating the consumption of H_2 through active oxygen species originating from Ag_2O. As TiO_2 does not release lattice oxygen, the observed consumption of H_2 is attributed solely to the presence of active oxygen on Ag_2O. To enhance the active oxygen generation and delivery abilities, Kim et al. [40] employed ceria as a promoter for Ag/TiO_2 in soot oxidation. The authors also reported H_2-TPR results for Ag supported on anatase between 250 °C and 330 °C, which resemble the reducibility characteristics of Ag/TiO_2 observed in our study. Ag supported on alumina (Ag/Al_2O_3) exhibited a single peak in the TCD signal at around 100 °C, indicating the presence of active oxygen -originating from Ag_2O. The reaction temperature was lower than 300 °C, and no reduction peaks were observed in the profiles of pure Al_2O_3, which confirms that the source of active oxygen is indeed Ag_2O. Ousji et al. [41] also investigated Ag-based catalysts on different supports for formaldehyde oxidation and used the H_2-TPR technique to determine the reduction of metal oxides. Their results showed that in the case of Ag/Al_2O_3, the peak TCD around 100 °C was caused by the presence of large Ag_2O.

Additionally, our study found that there was no catalyst-driven oxygen release at temperatures exceeding 150 °C, as evidenced by the absence of TCD signal peaks. This finding is consistent with Aneggi et al. [18], who used TPR to assess the reducibility of Ag-based catalysts and found that Ag has no effect on TPR traces of ZrO_2 and Al_2O_3. H_2-TPR analysis also showed no observable reduction peaks for Ag_xO, which confirms the presence of zero-valent Ag at temperatures >110 °C. Based on these experimental findings, it can be concluded that Ag_2O is fully converted to Ag^0 once it releases oxygen to H_2.

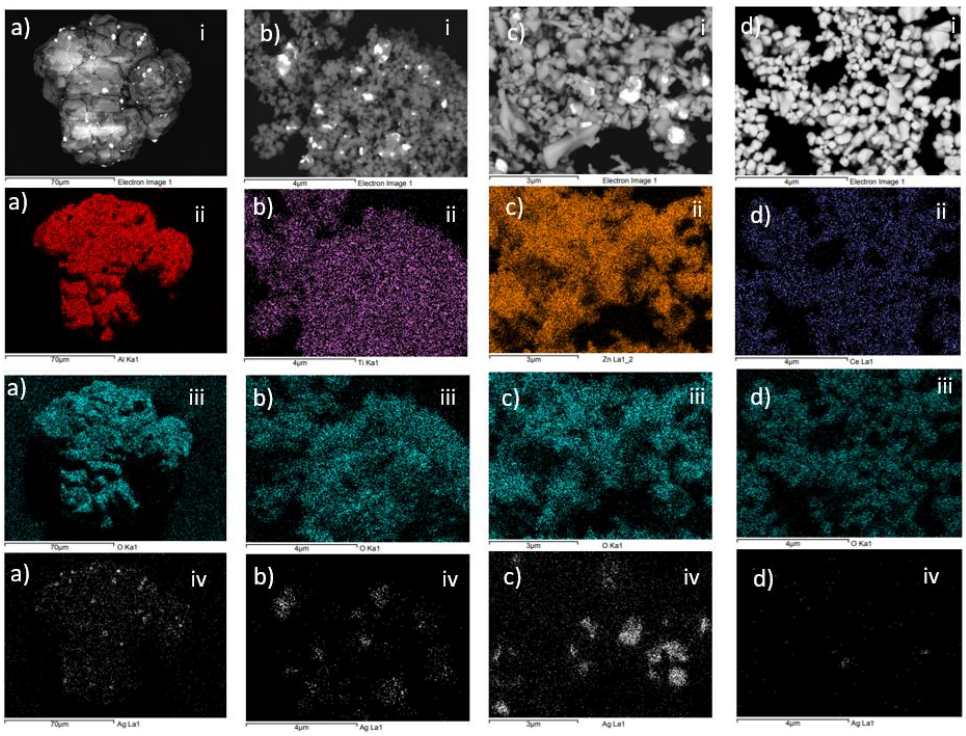

Fig. 2. SEM and SEM EDX images of a) Ag/Al_2O_3, b) Ag/ TiO_2, c) Ag/ZnO and Ag/ CeO_2. The number in fig 2 is a type of image as follows: SEM image (i), Type of the main element of supporter (ii) such as the image of Ag/ Al_2O_3 shows the Al, the element of oxygen (iii), and the element of silver (iv).

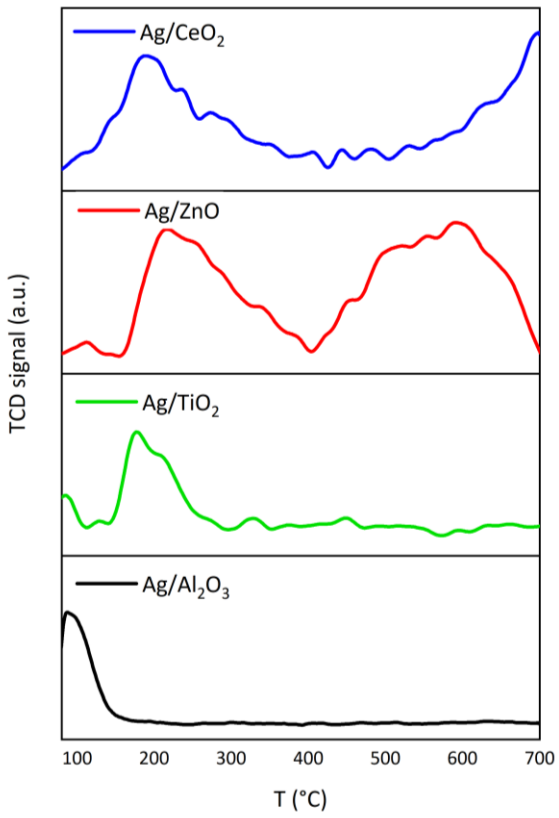

Fig. 3. H_2-TPR profiles of Ag/CeO_2, Ag/ZnO, Ag/TiO_2, and Ag/Al_2O_3 catalysts.

3.2 PM oxidation activity

3.2.1 Pure PM oxidation

Figure 4 shows the oxidation activity of pure PM and the percentage of weight loss, and the first derivative of weight loss (DTG) are shown in figure 4a and 4b, respectively. The combustion of PM is divided into three phases depending on its constituents: The initial combustion phase for light VOCs, the secondary combustion phase for heavy VOCs [11], and the final combustion phase for soot [32]. The phase of combustion is presented by DTG result.

Utilizing a 99.99% O_2 concentration, the DTG analysis exhibits three distinct peaks at 289 ºC, 389 ºC, and 517 ºC, which correspond to the oxidation of light VOCs, heavy VOCs, and soot, respectively. In the case of a 10 vol% O_2 in N_2 concentration, two peaks of DTG are observed at 271 ºC (light VOCs) and approximately 600 ºC (heavy VOCs). Similarly, when a 5 vol% O_2 in N_2 concentration is employed, two peaks of DTG are observed at 266 ºC (light VOCs) and approximately 600 ºC (heavy VOCs). The TGA results indicated that the weight loss percentage of pure PM was affected by the oxygen concentration. Complete combustion of PM was achieved at 700 ºC when 99.99% oxygen concentration was used, whereas at 10% oxygen concentration, a residual mass of 20% was observed at the same temperature. Similarly, a residual mass of 40% was observed at 700 ºC when the oxygen concentration was further reduced to 5%. The residual mass observed in the

latter cases was due to the presence of soot resulting from incomplete PM combustion. The effect of oxygen concentration on the combustion of light VOCs was found to be insignificant, while the combustion of heavy VOCs and soot was significantly affected by the oxygen concentration.

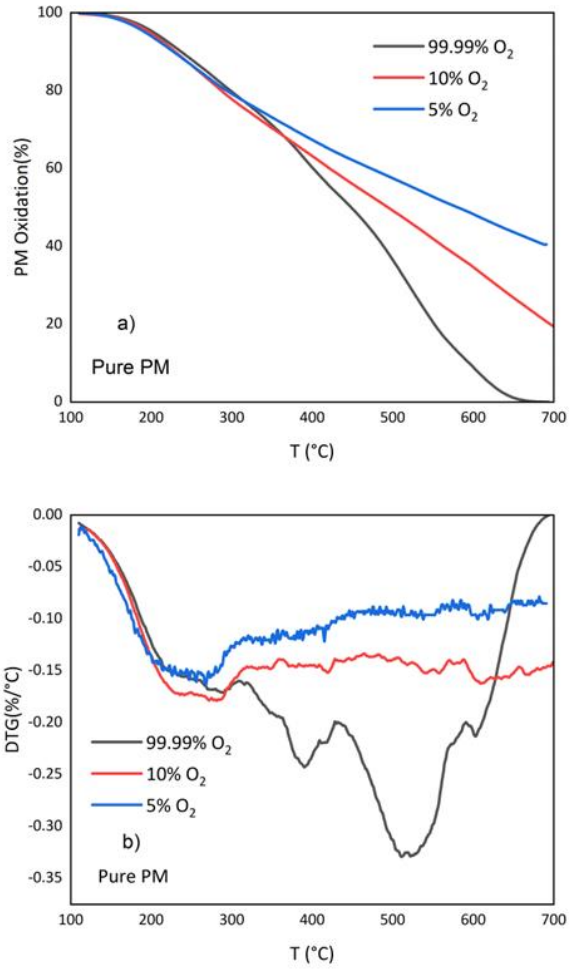

Fig. 4. Pure PM oxidation (a) and DTG of PM oxidation(b); using O_2 concentration 99.99% ,10% and 5 %.

3.2.2 PM with Ag/Al₂O₃

Figure 5 illustrates the PM oxidation activity of the Ag/Al_2O_3 catalyst. The weight loss percentage and the DTG curves are presented in figures 5a and 5b, respectively. The DTG peak of Ag/Al_2O_3 reveals two peaks at 251 ºC and 313 ºC in the presence of 99.99% O_2, while the presence of 10 vol% O_2 demonstrates peaks of DTG at 231 ºC and 341 ºC. The concentration of 5% oxygen exhibits the DTG peak at 215 ºC and 365ºC. The results of DTG indicate two phases of combustion. The first peak of DTG signifies the oxidation of light VOCs, while the second peak indicates the combustion of heavy VOCs and soot. Although the Ag/Al_2O_3 catalyst promotes active oxygen by Ag^0 after reaching a temperature of 300 ºC, the oxidation of light VOCs is not enhanced by the catalyst.

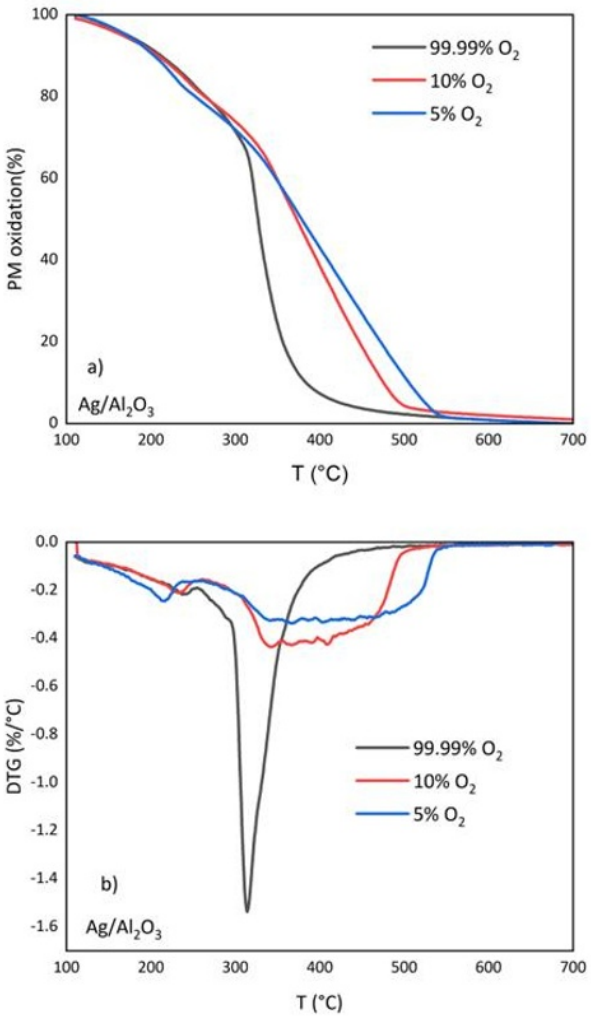

Fig. 5. a) PM oxidation b) DTG of PM oxidation; PM with Ag/Al_2O_3 and tight contact

In contrast, the combustion of heavy VOCs and soot is substantially promoted by Ag/Al_2O_3. The T_{20} values for Ag/Al_2O_3 when using 99.99%, 10%, and 5 vol % O_2 are 256, 264, and 253 ºC, respectively. The T_{20} value reflects the performance of the oxidation of light VOCs. The results of T_{20} demonstrate nuances of temperature, indicating that the concentration of oxygen has a low impact on the oxidation of light VOCs. The T_{55} values for Ag/Al_2O_3 when using 99.99%, 10%, and 5 vol % O_2 are 331, 385, and 394 ºC, respectively. The T_{55} value indicates the temperature required for the complete combustion of VOCs (heavy VOCs), which reflects the performance of VOCs combustion. It is observed that the reduction in oxygen concentration leads to an increase in the temperature required for the complete combustion of VOCs, implying that the VOCs combustion performance decreases as the oxygen concentration decreases in Ag/Al_2O_3 case. The T_{90} values for Ag/Al_2O_3 when using 99.99%, 10%, and 5 vol % O_2 are 384, 476, and 506 ºC, respectively. The T_{90} value represents the temperature required for the combustion of soot and reflects the performance of soot combustion. Similar to the trend observed for T_{55}, the results indicate that decreasing the

oxygen concentration leads to a decrease in the performance of soot combustion in the case of the Ag/Al_2O_3 catalyst.

3.2.3 PM with Ag/TiO_2

Figure 6 shows the PM oxidation activity of Ag/TiO_2, where the percentage of weight loss and DTG are displayed in figures 6a and 6b, respectively. The DTG of Ag/TiO_2 reveals two peaks at 197 °C and 425 °C in the presence of 99.99% O_2, while the presence of 10 vol% O_2 demonstrates peaks of DTG at 180 °C and 604 °C. Similarly, the concentration of 5% oxygen exhibits the DTG peak at 207 °C and 604°C. The results of DTG indicate two distinct phases of combustion, like Ag/Al_2O_3. Specifically, the first peak of DTG signifies the combustion of light VOCs, while the second peak indicates the combustion of heavy VOCs and soot. The Ag/TiO_2 catalyst promotes the combustion of light VOCs through the active oxygen generated by Ag_2O, as observed in the H_2-TPR results. This promotion of active oxygen leads to a lower temperature of oxidation of light VOCs compared to Ag/Al_2O_3.

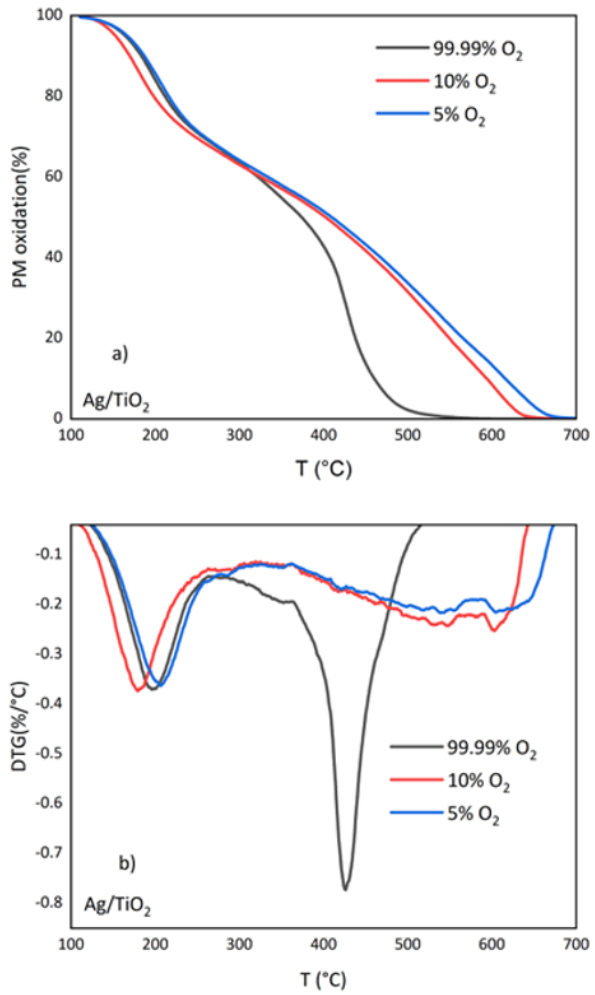

Fig. 6. a) PM oxidation b) DGT of PM oxidation; PM with Ag/TiO_2 and tight contact

Furthermore, the combustion of heavy VOCs and soot is promoted by Ag^0 after the temperature reaches 300 °C, resulting in a decrease in the temperature required for the combustion of heavy VOCs and soot. The T_{20} values for Ag/TiO_2 when using 99.99%, 10%, and 5 vol % O_2 are 212, 199, and 216 °C, respectively. The T_{20} values show a similar trend across different oxygen concentrations, indicating a weaker effect of varying oxygen concentration on the promotion of the combustion of light VOCs by Ag/TiO_2 T_{55} values for Ag/TiO_2 when using 99.99%, 10%, and 5 vol % O_2 are 394,432 and 440 °C, respectively. T_{55} in the case of Ag/TiO_2 shows a clear difference in temperature with a lower oxygen concentration. With this result, it can be implied that the performance of VOCs combustion decreases with less oxygen concentration. Furthermore, the effect of oxygen concentration on the activation of Ag/TiO_2 in promoting soot combustion is evident when considering T_{90}. The decrease in oxygen concentration from 99.99% to 10% results in a significant increase in the temperature required for soot combustion, with a difference of 133°C. The T_{90} values for Ag/TiO_2 when using 99.99%, 10%, and 5 vol % O_2 are 461, 594, and 616 °C, respectively. These results further emphasize the importance of oxygen concentration in promoting soot combustion using Ag/TiO_2.

3.2.4 PM with Ag/ZnO

Figure 7 illustrates the PM oxidation activity of Ag/ZnO, where figure 7a and 7b display the percentage of weight loss and DTG, respectively. In the presence of 99.99% O_2, Ag/ZnO displays three peaks of DTG at 174 °C, 350 °C and 414 °C. Conversely, the presence of 10 vol% O_2 demonstrates peaks of DTG at 174 °C, 415 °C, and 495 °C. Likewise, the concentration of 5% oxygen exhibits the DTG peak at 174 °C, 415 °C, and 542 °C. The results of the DTG analysis for Ag/ZnO showed three peaks. indicating the oxidation of light and heavy VOCs, as well as soot. The reduction of Ag_2O on Ag/ZnO was observed through H_2-TPR, which occurred at 150-400 °C, and suggested that the active oxygen from Ag_2O was responsible for the oxidation of light and heavy VOCs. The combustion of soot was found to occur after the oxidation of VOCs at temperatures between 450-550 °C. Additionally, lattice oxygen was released from ZnO at 400-700 °C, serving as an oxidizer. The reduction of Ag_2O by VOCs generated metallic silver, which acted as an active site for gas-phase oxygen to adsorb on Ag^0, facilitating the oxidation of soot on Ag/ZnO through either lattice or gas-phase oxygen. The T_{20} values of Ag/ZnO for different oxygen concentrations (99.99%, 10%, and 5 vol % O_2) were 172, 172, and 173°C, respectively. The almost similar T_{20} results for different oxygen concentrations indicate that oxygen concentration has a comparably smaller impact on mild VOC combustion by Ag/ZnO. T_{55} values for Ag/ZnO when using 99.99%, 10%, and 5 vol % O_2 are 377,406 and 409, respectively. The value of T_{55} in the case of oxygen consumption at a concentration of 99.99% shows a smaller value. in the case of 10% and 5% oxygen

concentrations. This result shows a significant effect on oxygen in the complete combustion of VOCs when Ag/ZnO is used as a catalyst.

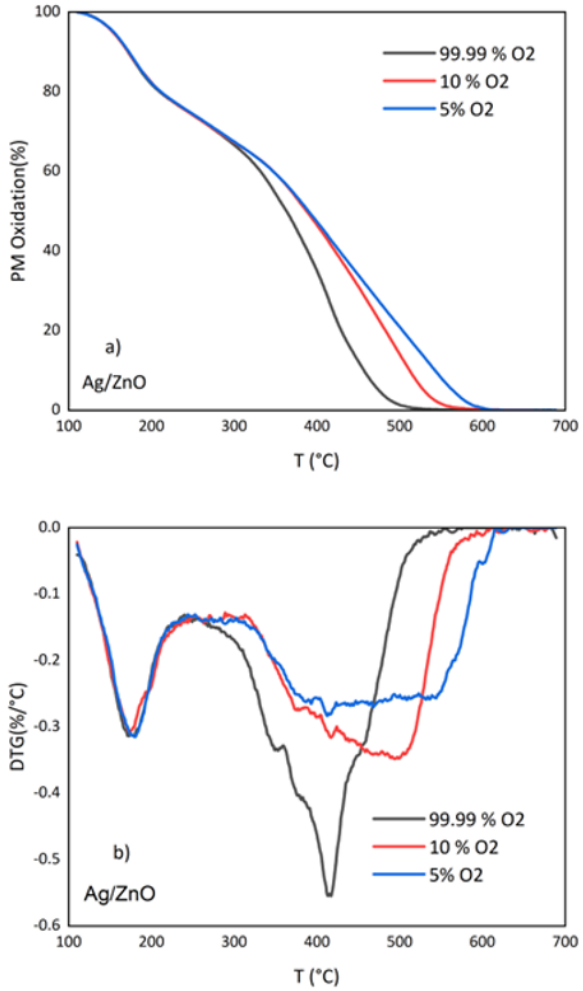

Fig. 7. a) PM oxidation b) DTG of PM oxidation; PM with Ag/ZnO and tight contact

It is of interest that in the case of Ag/ZnO shows similar performance of VOC oxidation in the case of 10 % and 5 % oxygen. concentrations. The T_{55} values for Ag/ZnO at oxygen concentrations of 99.99%, 10%, and 5 vol % are 377, 406, and 409, respectively. The T_{55} value at 99.99% oxygen concentration is smaller than those at 10% and 5% oxygen concentrations, indicating the significant effect of oxygen on the complete combustion of VOCs with Ag/ZnO catalyst. Notably, Ag/ZnO demonstrates comparable performance in VOC oxidation at 10% and 5% oxygen concentrations. The T_{90} values for Ag/ZnO under different oxygen concentrations were investigated, and the results show that the T_{90} values for 99.99%, 10%, and 5 vol % O_2 are 457°, 512°, and 543 °C, respectively. The T_{90} value is a measure of the temperature required for soot combustion and reflects the performance of the Ag/ZnO catalyst in promoting soot combustion. The trend observed for T_{90} is like that observed for T_{55}, indicating that a decrease in oxygen concentration leads to a decrease in the performance of soot combustion when using Ag/ZnO.

3.2.5 PM with Ag/CeO_2

Figure 8 presents the oxidation activity of Ag/CeO_2, with the weight loss percentage and the first derivative of weight loss (DTG) displayed in figures 8a and 8b, respectively. When exposed to a 99.99% O_2 atmosphere, Ag/CeO_2 exhibits three distinct DTG peaks at 180 °C, 317 °C, and 418 °C. Conversely, the presence of 10 vol% O_2 demonstrates peaks of DTG at 180 °C, 410 °C, and 497 °C. Likewise, the concentration of 5% oxygen exhibits the DTG peak at 180 °C, 416 °C, and 545 °C. DTG analysis revealed three distinct peaks corresponding to the oxidation of light and heavy VOCs, as well as soot, on Ag/CeO_2. H_2-TPR results indicated that active oxygen is removed from the Ag/CeO_2 surface at temperatures below 200 °C, while VOCs combustion occurs at higher temperatures. This suggests that active oxygen migrates from the catalyst surface to the particulate matter first, with catalytic burnout of VOCs occurring subsequently. Soot oxidation, on the other hand, is promoted by active values of Ag/CeO_2 were determined for different oxygen concentrations (99.99%, 10%, and 5 vol % O_2) were found to be 168, 171, and 169, respectively.

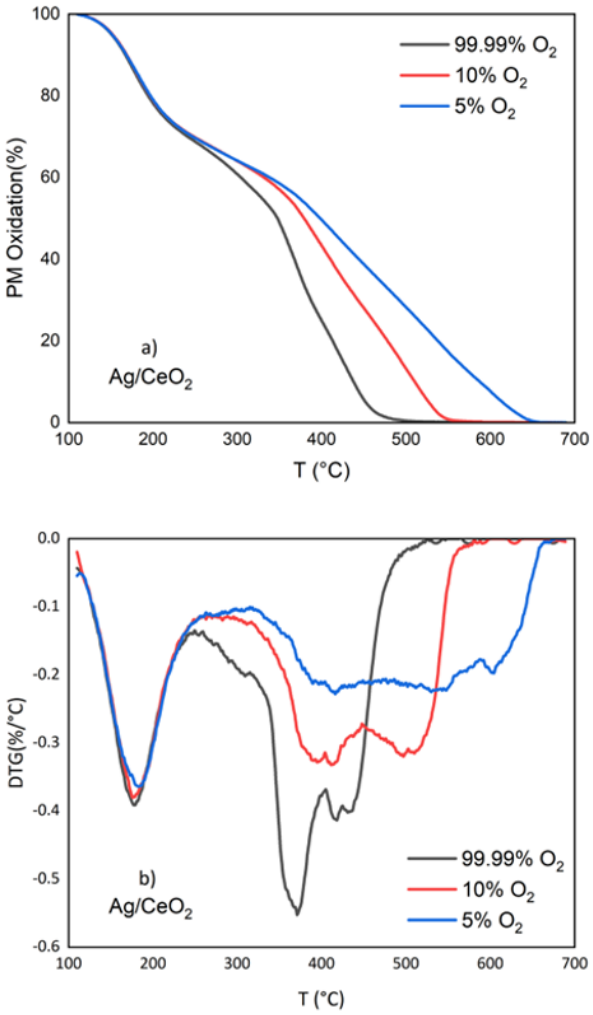

Fig. 8. a) PM oxidation b) DTG of PM oxidation; PM with Ag/CeO_2 and tight contact

The results of T_{20} show a nuanced temperature dependency. These findings suggest that changes in oxygen concentration have a low impact on the oxidation of light VOCs. T_{55} values for Ag/CeO_2 when using 99.99%, 10%, and 5 vol % O_2 are 359, 395 and 422 ºC, respectively. The T_{55} value of the case of Ag/CeO_2 shows an increase in the temperature with decreasing oxygen concentration, which affects the performance of the combustion of VOCs. Similarly, the T_{90} result indicates a decrease in soot oxidation performance for Ag/CeO_2 at low O_2 concentrations. The T_{90} values for 99.99%, 10%, and 5 vol % O_2 are 438, 511, and 588 ºC, respectively.

3.3 PM oxidation performance

3.3.1 the VOCs oxidation performances

Figure 9 illustrates the performance of VOC oxidation using Ag supported on different oxide materials and under different O_2 concentrations (99.99%, 10%, and 5%). When comparing the promotion effects of silver catalysts supported by different materials and utilizing a 99.99% oxygen concentration, the cumulative performance of VOCs (volatile organic compounds) combustion, in comparison to the pure PM case, can be summarized as follows: Ag/TiO_2 (7%), Ag/ZnO (11%), Ag/CeO_2 (15%), and Ag/Al_2O_3 (22%). Similarly, when employing a 10% oxygen concentration, the cumulative performance of VOCs combustion, relative to the pure PM case, for silver catalysts with different supporters can be summarized as: Ag/TiO_2 (6%), Ag/ZnO (11%), Ag/CeO_2 (14%), and Ag/Al_2O_3 (16%). Furthermore, when utilizing a 5% oxygen concentration, the comparative promotion effects of silver catalysts with different supporters on VOCs combustion, in relation to the pure PM case, can be summarized as: Ag/TiO_2 (17%), Ag/CeO_2 (20%), Ag/ZnO (22%), and Ag/Al_2O_3 (25%).

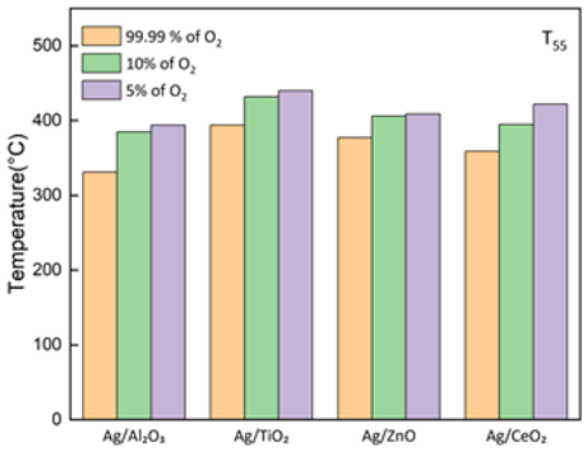

Fig. 9. The comparison of the VOCs oxidation performances.

3.3.2 the soot oxidation performances

In figure 10, the performance of soot oxidation using Ag supported on various oxide materials and subjected to different O_2 concentrations (99.99%, 10%, and 5%) is depicted. When comparing the promotional effects of silver catalysts supported by various materials and employing a 99.99% oxygen concentration, the overall performance of soot combustion, in relation to the pure PM case, can be succinctly summarized as follows: Ag/TiO_2 (23%), Ag/ZnO (23%), Ag/CeO_2 (26%), and Ag/Al_2O_3 (35%). Likewise, by utilizing a 10% oxygen concentration, the cumulative promotion of VOCs combustion, relative to the pure PM case, for silver catalysts with distinct supporters can be summarized as: Ag/TiO_2 (23%), Ag/ZnO (34%), Ag/CeO_2 (34%), and Ag/Al_2O_3 (38%). Furthermore, when employing a 5% oxygen concentration, the comparative effects of silver catalysts with diverse supporters on VOCs combustion, in relation to the pure PM case, can be concisely summarized as: Ag/TiO_2 (32%), Ag/CeO_2 (35%), Ag/ZnO (40%), and Ag/Al_2O_3 (44%). The results obtained using 99.99% O_2 show that Ag/Al_2O_3 exhibits the highest performance of soot oxidation, whereas Ag/TiO_2, Ag/ZnO, and Ag/CeO_2 demonstrate similar soot oxidation performances. When 10% and 5% O_2 are employed, the order of soot oxidation performance is $Ag/Al_2O_3 > Ag/ZnO > Ag/CeO_2 > Ag/TiO_2$.

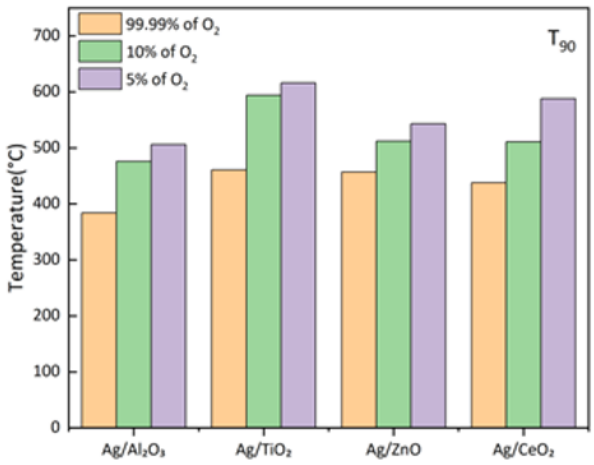

Fig. 10. The comparison of the soot oxidation performances.

4 Conclusions

The aim of this study was to investigate the impact of different oxygen concentrations (99.99%, 10%, and 5%) on the performance of PM oxidation using silver catalysts on various oxide supports. The results showed that the various oxygen concentrations had a minor effect on the combustion performance of light VOCs when compared to using no catalyst or the same catalyst. However, the combustion of heavy VOCs and soot, which require a higher oxygen concentration, significantly reduced the combustion performance. These findings indicate the importance of considering the oxygen concentration when selecting a catalyst for PM oxidation.

Acknowledgements

This research was funded by National Science, Research and Innovation Fund (NSRF), and King Mongkut's University of Technology North Bangkok with Contract no. KMUTNB-FF-66-19. P.Promhouad thanks King Mongkut's University of Technology, North Bangkok, and the National Science and Technology Development Agency, Thailand. Contract No. Grad 018/2563, for supporting his scholarship.

References

1. P.K. Wong, M.A. Ghadikolaei, S.H. Chen, A.A. Fadairo, K.W. Ng, S.M.Y. Lee, J.C. Xu, Z.D. Lian L. Li, H.C. Wong, Z. Ning, Physical, chemical, and cell toxicity properties of mature/aged particulate matter (PM) trapped in a diesel particulate filter (DPF) along with the results from freshly produced PM of a diesel engine, Journal of Hazardous Materials, **434** (2022): 128855
2. Q. Zhang, X. Meng, S. Shi, L. Kan, R. Chen, H. Kan, Overview of particulate air pollution and human health in China: Evidence, challenges, and opportunities, The Innovation, **3**,6 (2022): 0312
3. M. Lapuerta, J. Rodríguez-Fernández, J. Sánchez-Valdepeñas, Soot reactivity analysis and implications on diesel filter regeneration, Progress in Energy and Combustion Science, **78** (2020): 100833
4. L. Xiaowei, R. Jean-Charles, Y. Suyuan, Effect of temperature on graphite oxidation behavior, Nuclear Engineering and design, **227**,3 (2004): 273-280
5. Z. Li, W. Zhang, Z. Chen, Q. Jiang, Mechanism of accelerating soot oxidation by NO2 from diesel engine exhaust, Environmental Pollution, **264** (2020): 114708
6. M. Abián, C. Martín, P. Nogueras, J. Sánchez-Valdepeñas, J. Rodríguez-Fernández, M Lapuerta, M.U. Alzueta, Interaction of diesel engine soot with NO2 and O2 at diesel exhaust conditions. Effect of fuel and engine operation mode, Fuel, **212** (2018): 455-461
7. T.Y. Kim, S.H. LEE, Combustion and Emission Characteristics of Wood Pyrolysis Oil-Butanol Blended Fuels in a Di Diesel Engine, International Journal of Automotive Technology, **16** (2015): 903-912
8. F. Diehl, J. Barbier, D. Duprez, I. Guibard, G. Mabilon, Catalytic oxidation of heavy hydrocarbons over Pt/Al2O3. Oxidation of C10+ solid hydrocarbons representative of soluble organic fraction of Diesel soots, Applied Catalysis A: General, **504** (2015): 37-43
9. A.M. Gänzler, M. Casapu, F. Maurer, H. Störmer, D. Gerthsen, G. Ferre, P. Vernoux, B. Bornmann, R. Frahm, V. Murzin, M. Nachtegaal, Tuning the Pt/CeO2 Interface by in Situ Variation of the Pt Particle Size, Acs Catalysis, **8**,6 (2018): 4800-4811
10. X. Liang, X. Lv, Y. Wang, L. He, Y. Wang, K. Fu, Q. Liu, K. Wang, Experimental investigation of diesel soot oxidation reactivity along the exhaust after-treatment system components, Fuel, **302** (2021): 121047
11. B. Sawatmongkhon, K. Theinnoi, T. Wongchang, C. Haoharn, C. Wongkhorsub, E. Sukjit, A. Tsolakis, Catalytic oxidation of diesel particulate matter by using silver and ceria supported on alumina as the oxidation catalyst, Applied Catalysis A: General, **574** (2019): 33-40
12. J.H. Lee, D.Y. Jo, J.W. Choung, C.H. Kim, H.C. Ham, K.Y. Lee, Roles of noble metals (M = Ag, Au, Pd, Pt and Rh) on CeO2 in enhancing activity toward soot oxidation: Active oxygen species and DFT calculations, Journal of hazardous materials, **403** (2021): 124085
13. J.H. Lee, S.H. Lee, J.W. Choung, C.H. Kim, K.Y. Lee, Ag-incorporated macroporous CeO2 catalysts for soot oxidation: Effects of Ag amount on the generation of active oxygen species, Applied Catalysis B: Environmental, **246** (2019): 356-366
14. L. Zeng, L. Cui, C. Wang, W. Guo, C. Gong, Ag-assisted CeO2 catalyst for soot oxidation, Frontiers of Materials Science, **13** (2019): 288-295
15. C.M. Álvarez-Docio, R. Portela, J.J. Reinosa, F. Rubio-Marcos, J.F. Fernández, Pt mechanical dispersion on non-porous alumina for soot oxidation, Catalysis Communications, **140** (2020): 105999
16. H. Wang, S. Luo, X. Li, W. Liu, X. Wu, D. Weng, S. Liu, Thermally stable Ag/Al 2 O 3 confined catalysts with high diffusion-induced oxidation activity, Catalysis Today, **332** (2019): 189-194
17. E. Aneggi, J. Llorca, C. de Leitenburg, G. Dolcetti, A. Trovarelli, Soot combustion over silver-supported catalysts, **91**,1-2 (2009): 489-498
18. R. Camposeco, S. Castillo, M. Hinojosa-Reyes, N. Nava, R. Zanella, Manganese promoted TiO2 and ZrO2 nanostructures for soot combustion with boosted efficiency, Surface and Coatings Technology, **384** (2020): 125305
19. H.F. Wang, H.Y. Li, X.Q. Gong, Y.L. Guo, G.Z. Lu, P. Hu, Oxygen vacancy formation in CeO 2 and Ce 1-xZr xO 2 solid solutions: Electron localization, electrostatic potential and structural relaxation, Physical Chemistry Chemical Physics, **14**,48 (2012): 16521-16535
20. M. Wang, Y. Zhang, Y. Yu, W. Shan, H. He, Surface oxygen species essential for the catalytic activity of Ce-M-Sn (M = Mn or Fe) in soot oxidation, Catalysis Science & Technology, **11**,3 (2021): 895-903
21. E. Aneggi, C. de Leitenburg, G. Dolcetti, A. Trovarelli, Promotional effect of rare earths and transition metals in the combustion of diesel soot over CeO2 and CeO2-ZrO2, Catalysis Today, **114**,1 (2006): 40-47
22. K.I. Shimizu, H. Kawachi, A. Satsuma, Study of active sites and mechanism for soot oxidation by

silver-loaded ceria catalyst, Applied Catalysis B: Environmental, **96**,1-2 (2010): 169-175

23. X. Zhao, J. Jiang, H. Zuo, G. Jia, Soot combustion characteristics of oxygen concentration and regeneration temperature effect on continuous pulsation regeneration in diesel particulate filter for heavy-duty truck, Energy, **264** (2023): 126265
24. M. Debia, C. Couture, P.E. Njanga, E. Neesham-Grenon, G. Lachapelle, H. Coulombe, S. Hallé, S. Aubin, Diesel engine exhaust exposures in two underground mines, International Journal of Mining Science and Technology, **27**, 4 (2017): 641-645
25. H. Kopseak, Z. Pandur, M. Bačić, Ž. Zečić, H. Nevečerel, K. Lepoglavec, M. Šušnjar, Exhaust Gases from Skidder ECOTRAC 140 V Diesel Engine, Forests, **13**, 2 (2022): 272
26. B. Aliyu, D. Shitanda, S. Walker, B. Agnew, S. Masheiti, R. Atan, Performance and exhaust emissions of a diesel engine fuelled with Croton megalocarpus (musine) methyl ester, Applied Thermal Engineering, **31**,1 (2011): 36-41
27. I. A. Reşitoɔlu, K. Altinişik, A. Keskin, The pollutant emissions from diesel-engine vehicles and exhaust aftertreatment systems, Clean Technologies and Environmental Policy, **17** (2015): 15-27
28. G. Corro, E. Vidal, S. Cebada, U. Pal, F. Bañuelos, D. Vargas, E. Guilleminot, Electronic state of silver in Ag/SiO2 and Ag/ZnO catalysts and its effect on diesel particulate matter oxidation: An XPS study, Applied Catalysis B: Environmental, **216** (2017): 1-10
29. R. Prasad, S.V. Singh, A review on catalytic oxidation of soot emitted from diesel fuelled engines, Journal of Environmental Chemical Engineering, **8**,4 (2020): 103945
30. M. Skaf, S. Aouad, S. Hany, R. Cousin, E. Abi-Aad, A. Aboukaïs, Physicochemical characterization and catalytic performance of 10% Ag/CeO2 catalysts prepared by impregnation and deposition-precipitation, Journal of catalysis, **320** (2014): 137-146
31. H. Ruan, Soot oxidation performance with a HZSM-5 supported Ag nanoparticles catalyst and the characterization of Ag species, Rsc Advances, **7**,69 (2017): 43789-43797
32. G. Corro, S. Cebada, U. Pal, J.L.G. Fierro, J. Alvarado, Hydrogen-reduced Cu/ZnO composite as efficient reusable catalyst for diesel particulate matter oxidation, Applied Catalysis B: Environmental, **165** (2015): 555-565
33. L. Zhao, Y. Zhang, S. Bi, Q. Liu, Metal-organic framework-derived CeO2-ZnO catalysts for C3H6-SCR of NO: An: in situ DRIFTS study, RSC advances, **9**,33 (2019): 19236-19242
34. M. J. Kim, CeO2 promoted Ag/TiO2 catalyst for soot oxidation with improved active oxygen generation and delivery abilities, Journal of hazardous materials, **384** (2020): 121341
35. R. Ousji, Z. Ksibi, A. Ghorbel, C. Fontaine, Ag-Based Catalysts in Different Supports: Activity for Formaldehyde Oxidation, Advances in Materials Physics and Chemistry, **12**,08 (2022): 163-176